

RESEARCH ARTICLE

Open Access

# Mapping of the minimal inorganic phosphate transporting unit of human PiT2 suggests a structure universal to PiT-related proteins from all kingdoms of life

Pernille Böttger<sup>1,2,4</sup> and Lene Pedersen<sup>1,2,3\*</sup>

## Abstract

**Background:** The inorganic ( $P_i$ ) phosphate transporter (PiT) family comprises known and putative  $Na^+$ - or  $H^+$ -dependent  $P_i$ -transporting proteins with representatives from all kingdoms. The mammalian members are placed in the outer cell membranes and suggested to supply cells with  $P_i$  to maintain house-keeping functions. Alignment of protein sequences representing PiT family members from all kingdoms reveals the presence of conserved amino acids and that bacterial phosphate permeases and putative phosphate permeases from archaea lack substantial parts of the protein sequence when compared to the mammalian PiT family members. Besides being  $Na^+$ -dependent  $P_i$  ( $NaP_i$ ) transporters, the mammalian PiT paralogs, PiT1 and PiT2, also are receptors for gamma-retroviruses. We have here exploited the dual-function of PiT1 and PiT2 to study the structure-function relationship of PiT proteins.

**Results:** We show that the human PiT2 histidine, H<sub>502</sub>, and the human PiT1 glutamate, E<sub>70</sub>, - both conserved in eukaryotic PiT family members - are critical for  $P_i$  transport function. Noticeably, human PiT2 H<sub>502</sub> is located in the C-terminal PiT family signature sequence, and human PiT1 E<sub>70</sub> is located in ProDom domains characteristic for all PiT family members.

A human PiT2 truncation mutant, which consists of the predicted 10 transmembrane (TM) domain backbone without a large intracellular domain (human PiT2 $\Delta$ R<sub>254</sub>-V<sub>483</sub>), was found to be a fully functional  $P_i$  transporter. Further truncation of the human PiT2 protein by additional removal of two predicted TM domains together with the large intracellular domain created a mutant that resembles a bacterial phosphate permease and an archaeal putative phosphate permease. This human PiT2 truncation mutant (human PiT2 $\Delta$ L<sub>183</sub>-V<sub>483</sub>) did also support  $P_i$  transport albeit at very low levels.

**Conclusions:** The results suggest that the overall structure of the  $P_i$ -transporting unit of the PiT family proteins has remained unchanged during evolution. Moreover, in combination, our studies of the gene structure of the human PiT1 and PiT2 genes (*SLC20A1* and *SLC20A2*, respectively) and alignment of protein sequences of PiT family members from all kingdoms, along with the studies of the dual functions of the human PiT paralogs show that these proteins are excellent as models for studying the evolution of a protein's structure-function relationship.

## Background

Phosphate is needed by any living cell for structural and metabolic purposes. Inorganic phosphate ( $P_i$ ) has to be actively transported across the cell membrane against a chemical and electrical gradient. In mammalian cells

this task is managed by the type III sodium-dependent  $P_i$  ( $NaP_i$ ) symporters, PiT1 and PiT2, which utilize the free energy provided by the  $Na^+$  concentration gradient as the driving force for uphill import of  $P_i$ [1-3], reviewed in [4].

The mammalian type III transporters are part of the  $P_i$  transport (PiT) family (SLC20 [5]; TC #2.A.20 [6]), but several members were originally identified as receptors for different retroviruses belonging to the gamma-

\* Correspondence: LP@mb.au.dk

<sup>1</sup>Department of Molecular Biology, Aarhus University, C. F. Møllers Allé 3, Aarhus C, DK-8000, Denmark

Full list of author information is available at the end of the article

retrovirus genus [7-13]; thus, PiT1 and PiT2 are proteins with dual functions. The PiT family also comprises non-mammalian members, e.g., fungus Pho-4<sup>+</sup> (*Neurospora crassa* (*N. crassa*)) [14] and yeast Pho89 (*Saccharomyces cerevisiae* (*S. cerevisiae*)) [15] as well as the proton (H<sup>+</sup>)-dependent P<sub>i</sub> transporters from bacteria, PiTA and PiTB (*Escherichia coli* (*E. coli*)) [16], and plant Pht2\_1 (*Arabidopsis thaliana* (*A. thaliana*)) [17]. Furthermore, there is an increasing number of entries in the National Center for Biotechnology Information (NCBI) protein database (URL: <http://www.ncbi.nlm.nih.gov/>) that show similarity to the known members of the PiT family and therefore are denoted putative phosphate permeases; and PiT family members have been found in all kingdoms [18], reviewed in [19]. Altogether, this suggests that the PiT proteins developed very early in evolution and that this family of proteins has important function(s) in all kingdoms of life.

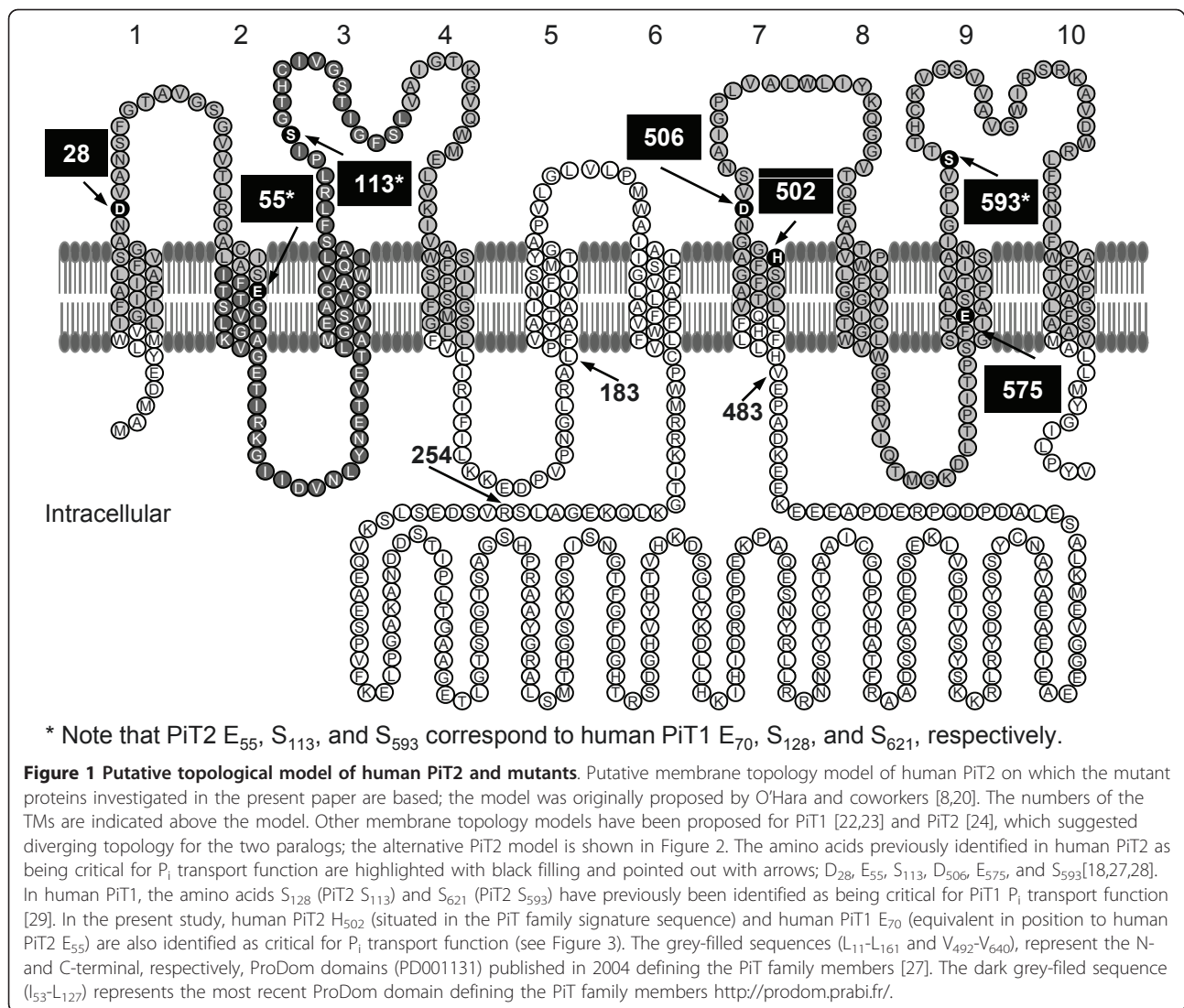
The first membrane topology model of PiT proteins was based on Kyte-Doolittle hydropathy plots. Analyses of human PiT1 and Pho-4<sup>+</sup> protein sequences predicted 10 transmembrane (TM) domains, 9 loops (here referred to as L1 to L9) hereof 5 extracellular, internal N- and C-terminal ends, and a large hydrophilic domain (L6) intracellularly positioned between the putative 6<sup>th</sup> and 7<sup>th</sup> TM domains [20]. Due to profound similarity (approx. 62% amino acid identity) between the human PiT paralogs, the same membrane topology model was proposed to also apply for human PiT2 (Figure 1) [8]. The model was, moreover, supported by the experimental assignment of the large intracellular domain of rat PiT2 to the cytoplasmic space [21]. Other topology models have, however, been proposed for PiT1 [22,23] and PiT2 [24] (Figure 2); please see legend to Figure 2 for more details. Nevertheless, we have shown that exchanging as little as 12 or 15 amino acids in the fungal PiT protein, Pho-4<sup>+</sup>, with human PiT1 or human PiT2 sequences, respectively, results in proteins that support infection by human PiT1 or PiT2 cognate gamma-retroviruses [25,26]; results, which suggest that these transporters are structurally highly related.

Analyzing human PiT1 and Pho-4<sup>+</sup> sequences, Johann and coworkers discovered an internal sequence repeat, which they suggested had originated from an ancient gene duplication [20]. Both regions were shown to harbor a ProDom domain, PD001131 (Figure 1) [27] (human PiT2 I<sub>11</sub>-L<sub>161</sub> and V<sub>492</sub>-V<sub>640</sub>), characteristic for all members of the PiT family. Interestingly, all amino acids in human PiT2 (i.e. D<sub>28</sub>, E<sub>55</sub>, S<sub>113</sub>, D<sub>506</sub>, E<sub>575</sub>, and S<sub>593</sub>) and in human PiT1 (S<sub>128</sub> and S<sub>621</sub>) identified to be critical for P<sub>i</sub> transport function are located in these ProDom domains (Figure 1) [18,27-29]. It should be noted, that, the ProDom domain PD001131 has changed and now consists of what corresponds to human PiT2

I<sub>53</sub>-L<sub>127</sub> <http://prodom.prabi.fr> (Figure 1). In an attempt to narrow down a PiT family trait, Saier aligned the N-terminal protein sequences from 17 members representing all kingdoms [6,30]. The author noted the existence of an 11-amino-acid-long sequence in the N-terminal region containing the conserved core sequence [GANDVANA] and proposed it to be a signature sequence for the PiT family [6,30]. However, refined studies of the N- and C-termini of 109 protein sequences representing PiT family members from all kingdoms revealed that these proteins harbor a 12-amino-acid-long PiT family signature sequence - with the common core consensus sequence [GANDVANA] - within each of the PD001131 ProDom domains proposed in 2004 [18]. Furthermore, D<sub>28</sub> and D<sub>506</sub> shown to be critical for PiT2 P<sub>i</sub> transport are placed in either of the PiT family signature sequences [18].

To further investigate the importance of the PiT family signature sequences, we have analyzed the human PiT2 histidine, H<sub>502</sub>, located in the C-terminal PiT family signature sequence, and we show that it is indeed critical for the P<sub>i</sub> transport function but dispensable for infection by PiT2 cognate gamma-retroviruses. The human PiT2 H<sub>502</sub> is the second amino acid in this sequence to be identified as critical for P<sub>i</sub> transport function. In addition, we also show that the human PiT1 glutamate, E<sub>70</sub>, located in the PD001131 ProDom domain, is critical for the P<sub>i</sub> transport function but dispensable for infection by PiT1 cognate gamma-retroviruses.

We have, moreover, combined studies of the gene structure of the human PiT genes (*SLC20A1* and *SLC20A2*), alignment and TM domain prediction of protein sequences of PiT family members from all kingdoms of life, and studies of the dual functions of the human PiT paralogs as P<sub>i</sub> transporters and gamma-retroviral receptors, and we found that these proteins are excellent as models for studying the evolution of protein structure-function relationship. Specifically based on the observation that bacterial and archaeal PiT family members are substantially smaller than eukaryotic members [18] and our alignment (Additional File 1 Figure A), we analyzed truncation mutants of human PiT2. Our results clearly show that the large intracellular domain of human PiT2 is dispensable for P<sub>i</sub> transport function, and that a fully functional P<sub>i</sub>-transporting unit can be created by the 10 TM domains and the small loop sequences connecting them (human PiT2ΔR<sub>254</sub>-V<sub>483</sub>). A further truncated human PiT2 protein with the 5<sup>th</sup> and 6<sup>th</sup> TM domains and the large intracellular domain removed resembles the structures of as well a putative phosphate permease from archaea as of PiTA from bacteria (*Archaeoglobus fulgidus* (*A. fulgidus*) and *E. coli*, respectively). This mutant (human PiT2ΔL<sub>183</sub>-V<sub>483</sub>) was



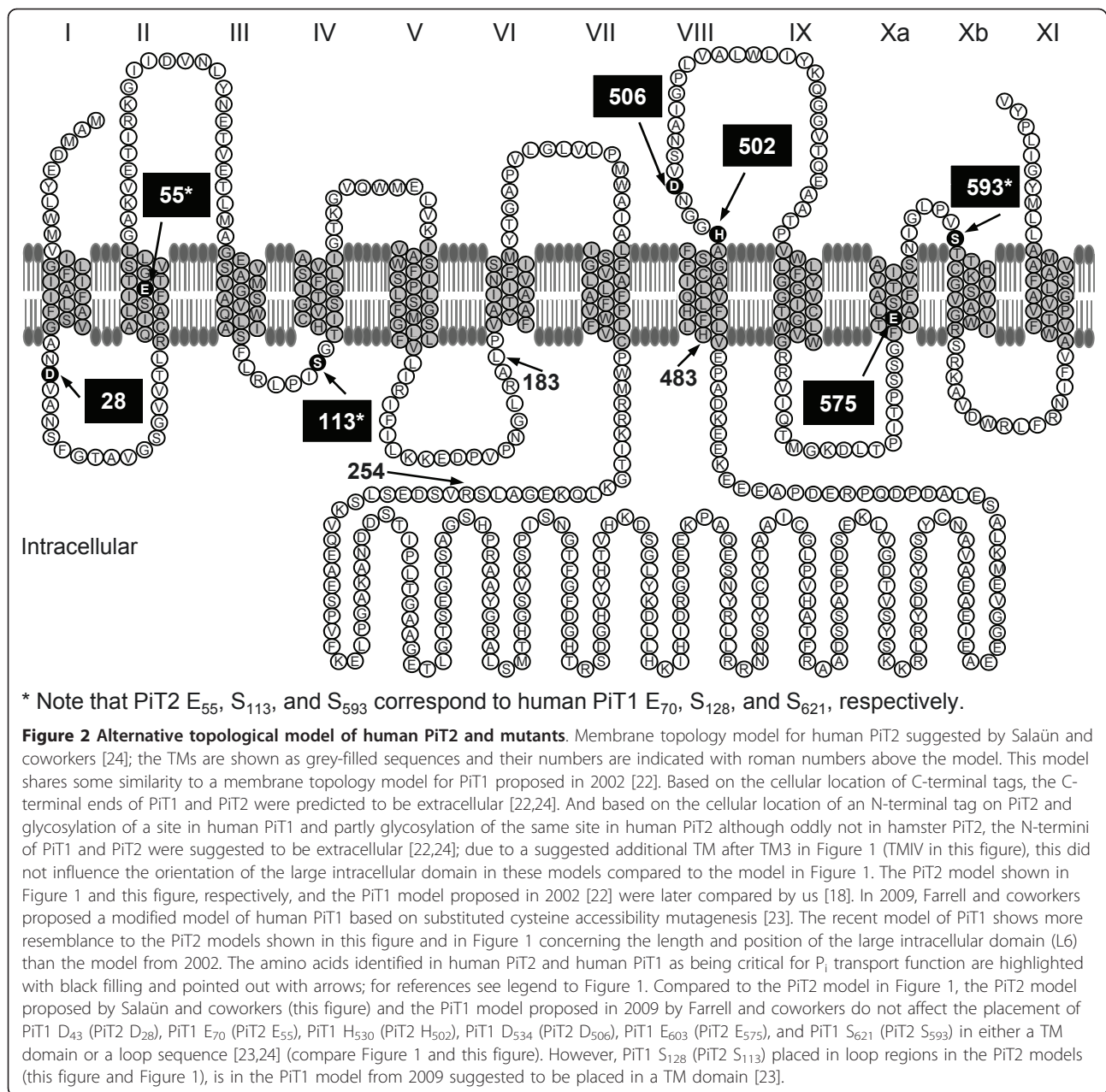
an excellent gamma-retroviral receptor [31], and we here show that it can support low levels of P<sub>i</sub> transport. Altogether, these results suggest that the overall structure of the P<sub>i</sub>-transporting unit of the PiT family proteins has remained unchanged during evolution.

## Methods

### Sequence alignment

Protein sequence alignment of nine PiT family members representing all kingdoms was made using the ClustalW alignment program version 2.0.12 available at the European Bioinformatics Institute server (URL: <http://www.ebi.ac.uk/clustalw2/>) [32]. The Swiss-Prot protein sequences were retrieved from the NCBI Protein server (URL: <http://www.ncbi.nlm.nih.gov/protein/>). Accession numbers are: *Homo sapiens* (*H. sapiens*) PiT2 [Swiss-Prot:Q08357], *H. sapiens* PiT1 [Swiss-Prot:Q08344], *Caenorhabditis elegans* (*C. elegans*) putative phosphate

permease [Swiss-Prot:Q17455], *Drosophila melanogaster* (*D. melanogaster*) putative phosphate permease [Swiss-Prot:Q9VTG0], *N. crassa* Pho-4<sup>+</sup> [Swiss-Prot:P15710], *Trypanosoma brucei* (*T. brucei*) putative phosphate permease [Swiss-Prot:Q9N930], *A. fulgidus* putative phosphate permease [Swiss-Prot:O29467], *A. thaliana* Pht2\_1 [Swiss-Prot:Q38954], and *E. coli* PiTA [Swiss-Prot:P37308]. All sequences encompass two 12-amino-acid-long sequences, which based on comparison of 109 sequences, were identified in PiT proteins and related proteins and suggested to be PiT family signature sequences [18]. We, however, observed that the C-terminal PiT family signature sequence of *E. coli* PiTA did not group together with the C-terminal PiT family signature sequences of the eight other species in the alignment (data not shown). In order to group all the C-terminal PiT family signature sequences together, the alignment was adjusted manually after an alignment of



*H. sapiens* PiT2 amino acids S<sub>422</sub>-V<sub>652</sub> [Swiss-Prot: Q08357], *A. fulgidus* putative phosphate permease [Swiss-Prot: O29467], and *E. coli* PiTA [Swiss-Prot: P37308]. For the adjusted protein sequence alignment of the PiT family members, see Additional File 1 Figure A.

#### Prediction of TM domains in the PiT family members and related proteins

Putative TM domains were predicted using the TMHMM Server v. 2.0 available at the Center for Biological Sequence Analysis, Technical University of Denmark (URL: <http://www.cbs.dtu.dk/services/TMHMM/>),

and the Dense Alignment Surface (DAS) Transmembrane Prediction server available at the Stockholm Bioinformatics Center, Stockholm University (URL: <http://www.sbc.su.se/~miklos/DAS/>). TMHMM is based on a hidden Markov model (HMM) that is cyclic with seven types of states for helix core, helix caps on either side, loop on the cytoplasmic side, two loops for the non-cytoplasmic side, and a globular domain state in the middle of each loop [33], and DAS is based on low-stringency dot-plots of the query sequence against a collection of non-homologous membrane proteins using a previously derived special scoring matrix [34].

In general, the predictions using both servers correspond well to each other when compared (data not shown), however, the DAS server tends to predict shorter TM domains in agreement with the tendency for prokaryotic TM domains to be shorter in length when compared to the length of eukaryotic TM domains [35]. Therefore, we chose to use the DAS server over the TMHMM server when predicting TM domains in the prokaryotic protein sequences for *E. coli* PiTA and *A. fulgidus* putative phosphate permease. The predicted TM domains are shown in Additional File 1 Figure A.

#### Intron-exon border analysis of human PiT genes *SLC20A1* and *SLC20A2*

The SPIDEY mRNA-to-genome DNA alignment program version 1.40 available from the NCBI homepage (URL: <http://www.ncbi.nlm.nih.gov/spidey/index.html>) [36] was used to determine the location of intron-exon borders in the human PiT genes. SPIDEY takes as input an mRNA sequence and the corresponding genomic sequence, and it generates an alignment that establishes the gene structure. The GenBank mRNA sequences were retrieved from the NCBI nucleotide server (<http://www.ncbi.nlm.nih.gov/nuccore/>). Accession numbers are: *H. sapiens* PiT1 mRNA [GenBank:NM\_005415] and *H. sapiens* PiT2 mRNA [GenBank:NM\_006749]. The genomic GenBank sequences were retrieved from the NCBI human genome server (<http://www.ncbi.nlm.nih.gov/projects/genome/guide/human/>). Accession numbers are: *H. sapiens* chromosome 2 (*SLC20A1*) [GenBank:NC\_000002] and *H. sapiens* chromosome 8 (*SLC20A2*) [GenBank:NC\_000008]. The intron-exon borders are shown in Additional File 1 Figure A on the protein sequence alignment of nine PiT family members.

#### Expression plasmids

The pcDNA1A<sup>R</sup>tkpA-derived expression plasmids pOJ74 and pOJ75 (Wyeth-Ayerst Research, Pearl River N.Y., USA) encoding human PiT2 and PiT1, respectively, have been described [37].

The plasmid encoding the human PiT2 H<sub>502</sub>A mutant was made by using the QuickChange<sup>®</sup> XL site-directed mutagenesis kit (Stratagene, La Jolla CA, USA) according to the manufacturer's instructions. Besides the mutations creating H<sub>502</sub>A, the forward primer 5'-TTCGGGTCCTTTGCTGCCGCGGCAATGACGT-3' and reverse primer 5'-ACGTCATTGCCGCGGAGCAAAGGACCCGAA-3' also generated, by introduction of a silent mutation, an *Ngo*M IV restriction enzyme cleavage site in pOJ74, which was used for screening. The plasmid encoding the human PiT1 E<sub>70</sub>K mutant was made by using the Altered sites II kit (Promega, Madison WI, USA) according to the manufacturer's

instructions. A mutation creating E<sub>70</sub>K as well as a *Dra* I restriction enzyme cleavage site was introduced into a pAlter-1 vector (Promega) harboring the *Pst* I - *Hind* III fragment of pOJ75 (the nucleotide sequence encoding the N-terminal part of the human PiT1 protein) using the primer 5'-GACAGAGCCCACTGTTTAAA-GATGCTAGCTAG-3'. Finally, this construct was digested with *Kpn* I and *Hind* III generating a fragment, which was used to replace the corresponding fragment in pOJ75 resulting in the desired plasmid.

The plasmid encoding the human PiT2ΔL<sub>183</sub>-V<sub>483</sub> mutant has previously been described [31]. The plasmid encoding the human PiT2ΔR<sub>254</sub>-V<sub>483</sub> mutant was made using a pAlter-1 vector harboring the *Pst* I - *Hind* III fragment of pOJ74 (the nucleotide sequence encoding the N-terminal part of the human PiT2 protein) as template in a polymerase chain reaction (PCR) with the forward primer 5'CTATAGGGAGACCCAAGCTTTGTTTATTTAA3' and the reverse primer 5'GAGGACCTGGAGGAAATGGAACAGGAGGTGTGATAAAGCACC TTCTTTTGG3'; the latter primer was used to create the link between the 5' sequence encoding KEGALS<sub>253</sub> and the 3' sequence encoding H<sub>484</sub>LLFH (Figure 1). The amplification product was digested with *Sse* 8387 I and *Hind* III and used to replace the corresponding fragment in pOJ74 resulting in the desired plasmid.

The authenticities of all the nucleotide sequences were confirmed.

The plasmids were purified using either cesium chloride (CsCl) according to the protocol described by Maniatis and coworkers [38], or using Nucleobond (Macherey-Nagel, Düren, Germany) or Qiagen maxiprep (Qiagen GmbH, Hilden, Germany) according to the manufacturer's instructions.

#### Cell cultures

Chinese hamster ovary K1 cells, CHO K1 (ATCC CCL-61) and dog osteosarcoma cells, D17 (ATCC CCL-183), were cultivated as described [37]; *Mus dunni* tail fibroblasts, MDTF (ATCC CCL-2017) were cultivated in Dulbecco's modified Eagle's medium supplemented with 10% fetal bovine serum (FBS), 100IU per mL of penicillin (P), and 100 µg of streptomycin (S) per mL (D-MEM/FBS/PS). A-MLV (4070A isolate), 10A1 MLV, and Gibbon ape leukemia virus (GALV, SEATO) pseudotypes of the β-galactosidase-encoding transfer vector G1BgSvN [39] were obtained from the producer cell lines PA317GBN, PT67GBN, and PG13GBN, respectively [40-42]. PT67GBN was established as described [28]. All packaging cells were cultivated in DMEM supplemented with 10% newborn calf serum (NCS) and PS (D-MEM/NCS/PS). Feline leukemia virus subgroup B (FeLV-B) vector pseudotypes carrying the G1BgSvN transfer vector were made essentially as described [43].

Vectors were harvested as supernatants from confluent producer cells, and the vector containing supernatants were filtered (0.45- $\mu$ m pore size) and stored at -80°C.

#### Transient transfection and infection assay

Transient transfection-infection assays were performed essentially as described [37]. Briefly, CHO K1 cells seeded in 60-mm-diameter dishes at  $8 \times 10^4$  cells per dish were transfected with 2  $\mu$ g per dish of plasmid DNA encoding human PiT2 (pOJ74), human PiT1 (pOJ75), human PiT2 H<sub>502</sub>A, human PiT1 E<sub>70</sub>K, or equimolar amounts to human PiT2 of human PiT2 $\Delta$ R<sub>254</sub>-V<sub>483</sub> or human PiT2 $\Delta$ L<sub>183</sub>-V<sub>483</sub>. Mock treated cells were transfected with empty vector DNA (pcDNA1A<sup>R</sup>tkpA). Three independent precipitates were made per construct. Forty-eight hours after transfection, approx. 4 to  $8 \times 10^4$  10A1 MLV or A-MLV pseudotypes carrying the G1BgSvN transfer vector were added per dish in the presence of Polybrene. Forty-eight hours later, the dishes were stained and evaluated. Infection was analyzed by counting the number of  $\beta$ -galactosidase-positive (infected) cells per dish. Analyses for FeLV-B and GALV receptor functions were performed on MDTF cells using  $1.5 \times 10^4$  cells and approx.  $1.5$  to  $3.0 \times 10^4$  vector pseudotypes per dish. Numbers of vector pseudotypes used in the experiments were calculated from the number of  $\beta$ -galactosidase-positive colonies per mL obtained on D17 cells as described [37].

#### <sup>32</sup>P<sub>i</sub> transport assay

Female *Xenopus laevis* (*X. laevis*) frogs were obtained from Nasco (Nasco, Modesto CA, USA) and kept and handled according to guidelines from the Danish Animal Experiments Inspectorate. Oocytes were isolated from frogs anesthetized in a 0.1-0.2% MS.222 (3-amino-benzoic acid ethyl ester) (Sigma, St. Louis MO, USA) solution for 10-30 minutes. A 1-1.5 centimeters incision was made in the abdomen and several ovaries were removed surgically by authorized personnel. The oocytes were manually dissected and subsequently collagenase (Sigma, St. Louis MO, USA) treated and maintained in modified Barth's solution [88 mM NaCl, 1 mM KCl, 0.82 mM MgSO<sub>4</sub>, 0.4 mM CaCl<sub>2</sub>, 0.33 mM Ca(NO<sub>3</sub>)<sub>2</sub>, 2.4 mM NaHCO<sub>3</sub>, 10 mM HEPES-KOH, pH 7.5, 100 IU per mL penicillin, 100  $\mu$ g per mL streptomycin] at 18°C as described [28]. The following day, the oocytes were used for cRNA injection and subsequent analyses of <sup>32</sup>P<sub>i</sub> uptake essentially as described previously [28]. Briefly, cRNAs were prepared from *Apa* 1 (Figure 3A) or *Bln* 1 (Figures 3B and 6) linearized plasmid preparations applying the mMMESSAGE mMACHINE kit (Ambion, Austin TX, USA). Stage V-VI oocytes were microinjected with 12.5 ng of cRNA (or H<sub>2</sub>O as negative control) and incubated at 18°C. After two to three days, the

oocytes were washed in phosphate-free uptake solution [100 mM NaCl, 2 mM KCl, 1 mM CaCl<sub>2</sub>, 1 mM MgCl<sub>2</sub>, 10 mM HEPES-Tris pH 7.5], and hereafter incubated in uptake solution containing 0.1 mM KH<sub>2</sub><sup>32</sup>PO<sub>4</sub> (2 mCi per mL, New England Nuclear, Boston MA, USA) at RT for 1 hour. The oocytes were washed in ice-cold uptake solution containing 5 mM KH<sub>2</sub>PO<sub>4</sub> and the <sup>32</sup>P<sub>i</sub> uptake of each oocyte measured in a liquid scintillation counter as described previously [28]. It should be noted that factors coupled to the health and husbandry of the female *X. laevis* frogs can influence the oocyte batches. These factors include nutrition, season of the year (light cycle), water temperature, salinity and hardness of the water, water contaminants or toxins, and diseases [44], and the impact is that different batches of oocytes injected with cRNAs encoding the same proteins exhibit different average transport capacities.

#### Statistical analysis

The null hypothesis that two mean values are identical was tested by a two-tailed Student's *t*-test. The test compares the actual difference between two mean values in relation to the variation in the data (expressed as the standard error of the difference between the mean values). The null hypothesis was rejected, e.g., the mean values were considered different when *P*<0.05.

## Results and discussion

### Human PiT1 E<sub>70</sub> and human PiT2 H<sub>502</sub> are critical for P<sub>i</sub> transport function but dispensable for gamma-retroviral receptor function

In a former study, we identified the putative 2<sup>nd</sup>-TM domain-positioned human PiT2 E<sub>55</sub> as being critical for PiT2 P<sub>i</sub> transport function (Figure 1) [28]. The human PiT2 paralog, human PiT1, harbors a corresponding glutamate in position 70, E<sub>70</sub>. To investigate whether this conserved residue was important for PiT1 P<sub>i</sub> transport function, it was mutated to a lysine generating the mutant human PiT1 E<sub>70</sub>K. In the experiment shown in Figure 3A, oocytes injected with cRNA encoding human PiT1 supported a <sup>32</sup>P<sub>i</sub> uptake of 119.86  $\pm$  28.16 pmol/oocyte-hour at pH 7.5 in agreement with previous results obtained addressing the Na<sup>32</sup>P<sub>i</sub> uptake function of human PiT1 in *X. laevis* oocytes [45]. The P<sub>i</sub> transport function of human PiT1 E<sub>70</sub>K was severely impaired when compared to that of wildtype PiT1 (*P* = 0.002, 2.78  $\pm$  0.74 pmol/oocyte-hour (PiT1 E<sub>70</sub>K)) (Figure 3A); see Additional File 2 for data and statistics to Figure 3.

Besides being P<sub>i</sub>-transporting proteins, the mammalian PiT proteins also serve as gamma-retroviral receptors, and this dual-function allows for analyzing whether a mutated PiT protein is properly processed, folded and translocated to the cell surface [18,28]. The human PiT1

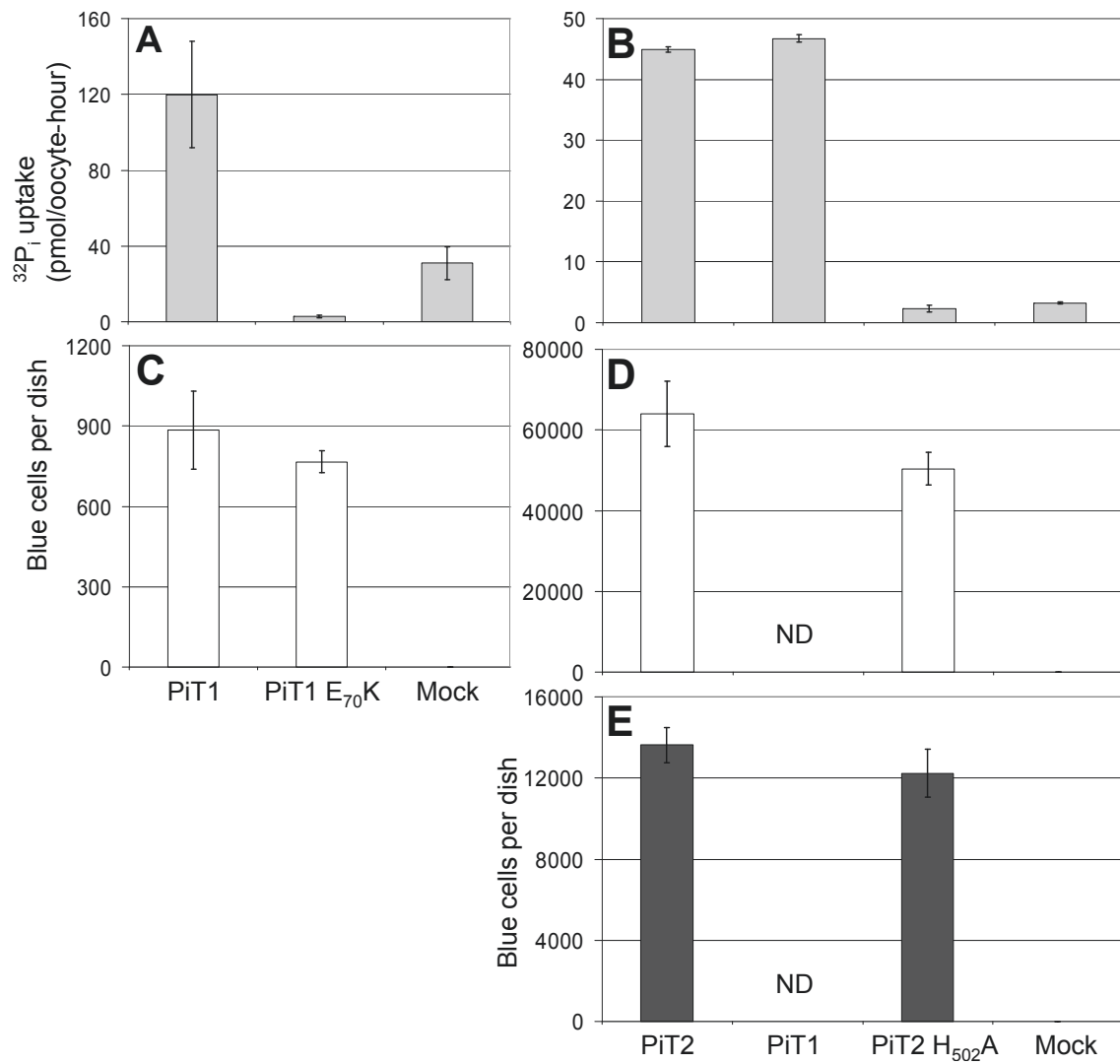


**Figure 3 Analysis of human PiT1 E<sub>70</sub>K and PiT2 H<sub>502</sub>A for Na<sup>32</sup>P<sub>i</sub> uptake and gamma-retroviral receptor function.** A-B *X. laevis* oocytes were injected with H<sub>2</sub>O (Mock) or cRNA of the indicated constructs. Three days later, a <sup>32</sup>P<sub>i</sub> uptake assay was performed and the <sup>32</sup>P<sub>i</sub> uptake in individual oocytes was measured. Data are the mean value of (n) numbers of oocytes ±SEM, see Additional File 2 for data and statistics. Experiments A and B were made independently of each other, and the experiments were repeated and similar results obtained. C CHO K1 cells were transfected with CsCl-purified PiT1- or PiT1 E<sub>70</sub>K-encoding plasmid or empty vector DNA (Mock). Three independent precipitates were made for each construct. Forty-eight hours after transfection, approx. 8 × 10<sup>4</sup> 10A1 MLV pseudotypes were added per dish. The average numbers (±SEM) of blue (infected) cells per dish from three dishes receiving independent precipitates are shown, see Additional File 2 for data and statistics. D-E were made in parallel using the same protocol as in (C) with the exception that Nucleobond-purified plasmids encoding PiT2, PiT2 H<sub>502</sub>A, or empty vector DNA were used. The dishes were challenged with approx. 4 × 10<sup>4</sup> 10A1 MLV pseudotypes (D) or A-MLV pseudotypes (E). The average numbers (±SEM) of blue (infected) cells per dish from three dishes receiving independent precipitates are shown, see Additional File 2 for data and statistics.

E<sub>70</sub>K mutant was therefore analyzed for gamma-retroviral receptor function using a transient transfection-infection assay [37]. For the infection assay, retroviral vectors harboring a β-galactosidase encoding transfer vector and carrying viral surface proteins responsible for receptor recognition were used; vectors carrying, e.g., 10A1 MLV surface proteins are referred to as 10A1 MLV vector pseudotypes. Eukaryotic expression

plasmids encoding human PiT1 and human PiT1 E<sub>70</sub>K mutant protein were transfected into CHO K1 cells non-permissive for infection by 10A1 MLV vector pseudotypes (Figure 3C) [28]. The abilities of these proteins to support infection by 10A1 MLV vector pseudotypes were analyzed; the infection levels were evaluated as the number of β-galactosidase positive (blue) cells per 60-mm-diameter dish. CHO K1 cells expressing human

PiT1 were permissive for infection by 10A1 MLV vector pseudotypes (Figure 3C) in agreement with PiT1's well-described receptor function for 10A1 MLV [10]. Moreover, the human PiT1 E<sub>70</sub>K mutant supported wildtype PiT1 levels of 10A1 MLV infection (884 ±146 blue cells per dish (PiT1), 767 ±42 blue cells per dish (PiT1 E<sub>70</sub>K),  $P = 0.48$ ) (Figure 3C). Besides being a receptor for 10A1 MLV, PiT1 is also a receptor for GALV [7] and for FeLV-B [13]. The human PiT1 E<sub>70</sub>K protein was analyzed in parallel for receptor function for vector pseudotypes of these two viruses in non-permissive *Mus dunni* tail fibroblasts and found to sustain wildtype PiT1 infection levels of GALV (2087 ±780 blue cells per dish (PiT1), 1992 ±273 blue cells per dish (PiT1 E<sub>70</sub>K),  $P = 0.91$ ) and FeLV-B (1424 ±346 blue cells per dish (PiT1), 1715 ±527 blue cells per dish (PiT1 E<sub>70</sub>K),  $P = 0.67$ ). The wildtype receptor functions of PiT1 E<sub>70</sub>K confirm that the overall membrane topology is preserved and that the processing to the cell surface was unaffected by the E<sub>70</sub>K-mutation.

The glutamate E<sub>70</sub> in human PiT1 is conserved in eukaryotic PiT family members as are the other two human PiT1 residues (S<sub>128</sub> and S<sub>621</sub>) (Additional File 1 Figure A) previously shown to be critical for P<sub>i</sub> transport function [29]. Since the corresponding glutamate and serine residues in human PiT2 have already been identified as being critical for P<sub>i</sub> transport function [27,28], this demonstrates that equivalent glutamate or serine residues in the human PiT paralogs both are critical for their P<sub>i</sub> transport functions. These observations illustrate that it is highly likely that the other conserved amino acids identified in human PiT2 as being critical for P<sub>i</sub> transport function also are important for the transport function of human PiT1 and other PiT family members.

The histidine residue, human PiT2 H<sub>502</sub> is positioned in the 7<sup>th</sup> TM domain according to the Johann topology model (Figure 1) [20]. It is, moreover, located in the C-terminal PiT family signature sequence and conserved in eukaryotic PiT family members [18] (Additional File 1 Figure A). Moreover, analysis of 60 sequences of bacterial PiT family members revealed only 5 sequences without the histidine residue illustrating that this residue is also highly preserved in the C-terminal PiT family signature sequence of PiT family members belonging to this kingdom [18] (Additional File 1 Figure A). Since the conserved aspartic acid in the C-terminal PiT family signature sequence, that is human PiT2 D<sub>506</sub>, is critical for P<sub>i</sub> transport of PiT2 [18], we hypothesized that other conserved amino acids in this motif might be critically involved in P<sub>i</sub> transport function of human PiT2 and other members of the PiT family as well. Mutation of human PiT2 H<sub>502</sub> to alanine created the mutant denoted PiT2 H<sub>502</sub>A. This mutant was analyzed for <sup>32</sup>P<sub>i</sub> transport function in *X. laevis* oocytes (Figure 3B) and 10A1 MLV

and A-MLV receptor functions in CHO K1 cells (Figures 3D-E).

In the experiment shown in Figure 3B, oocytes injected with cRNA encoding human PiT2 supported a <sup>32</sup>P<sub>i</sub> uptake of 44.96 ±0.46 pmol/oocyte-hour at pH 7.5 in agreement with former studies addressing the Na<sup>32</sup>P<sub>i</sub> uptake function of human PiT2 in *X. laevis* oocytes [18,28,45]. The Pi transport function of human PiT2 H<sub>502</sub>A was severely impaired when compared to that of wildtype PiT2 ( $P = 0.002$ , 2.36 ±0.56 pmol/oocyte-hour (PiT2 H<sub>502</sub>A)) (Figure 3B).

To analyze whether the human PiT2 H<sub>502</sub>A mutant is properly folded and processed to the cell surface, it was also analyzed for gamma-retroviral receptor function using the transient transfection-infection assay [37]. Eukaryotic expression plasmids encoding human PiT2 and human PiT2 H<sub>502</sub>A mutant protein were transfected into CHO K1 cells non-permissive for infection by A-MLV and 10A1 MLV vector pseudotypes (Figures 3D-E) [28,37]. CHO K1 cells expressing human PiT2 were permissive for infection by both A-MLV and 10A1 MLV vector pseudotypes (Figures 3D-E) in agreement with PiT2's well-described receptor function for A-MLV and 10A1 MLV [8,10,37]. Moreover, the human PiT2 H<sub>502</sub>A mutant supported wildtype PiT2 levels of 10A1 MLV infection (63,940 ±8076 blue cells per dish (PiT2), 50,408 ±4005 blue cells per dish (PiT2 H<sub>502</sub>A),  $P = 0.23$ ) (Figure 3D) and A-MLV infection (13,624 ±862 blue cells per dish (PiT2), 12,235 ±1189 blue cells per dish (PiT2 H<sub>502</sub>A),  $P = 0.48$ ) (Figure 3E). These results demonstrate that the overall membrane topology of human PiT2 H<sub>502</sub>A is preserved, and that the processing of human PiT2 H<sub>502</sub>A to the membrane surface is unaffected by the mutation. Thus, histidine 502 in the 7<sup>th</sup> TM domain is the second amino acid - besides D<sub>506</sub> - in the C-terminal PiT family signature sequence [HGANDVQNAIGP], which has been shown to be essential for human PiT2 P<sub>i</sub> transport function. While the exact role of the histidine residue in the C-terminal signature sequence still needs to be revealed, its critical role for human PiT2 P<sub>i</sub> transport function emphasizes the importance of the C-terminal PiT family signature sequence in the physiological function of the PiT proteins.

Besides human PiT1 E<sub>70</sub> and human PiT2 H<sub>502</sub>, six conserved amino acids in human PiT2 and two corresponding positions in human PiT1 have previously been identified as being critical for P<sub>i</sub> transport function [18,27-29]. All these amino acids are located in the Pro-Dom domains (PD001131) suggested in 2004 to define members of the PiT family (Figure 1) [27]. Therefore it is likely that sequences outside these two domains might be dispensable for the P<sub>i</sub> transport function of the PiT proteins, and that a minimal P<sub>i</sub>-transporting unit of the PiT proteins can be identified.



### Alignment of protein sequences of PiT family members from all kingdoms

A previously published alignment of human PiT1 and human PiT2 protein sequences shows that the L6 loop - the large intracellular domain - is the region where these sequences diverge the most [8] (Additional File 1 Figure A). Moreover, alignment of human PiT1 and *N. crassa* Pho-4<sup>+</sup> shows that the large intracellular domain (L6) is smaller in Pho-4<sup>+</sup>, whereas the rest of the Pho-4<sup>+</sup> protein sequence aligns well with the protein sequence of human PiT1 [20] (Additional File 1 Figure A). To further address this, we counted the number of amino acids in the large intracellular domain (L6) of nine different PiT family members and plotted the lengths according to their phylogenetic relationship in Figure 4A. The figure shows that PiT family members from archaea and bacteria harbor the shortest L6 loops whereas the PiT-proteins from chordates harbor the longest L6 loops (Figure 4A, see also Additional File 1

Figure A). Note that the L6 loop of the *C. elegans* putative phosphate permease is unexpectedly short (73 amino acids), and according to the plot we would have expected a L6 loop length for this protein in the interval between 175 and 232 amino acids (Figure 4A). The observed differences in the L6 loop lengths of PiT family members from different species thus suggest that the L6 loop evolved from being a regular loop to become a regular domain during evolution. In order to address this issue, we counted the number of amino acids in all loops (L1 to L9) in the nine PiT family members and plotted the average loop lengths  $\pm$ SEM in Figure 4B. The figure shows that the L6 loop in average is much larger than all other loops (L6:  $>131.7 \pm 32.8$  amino acids, Figure 4B); see Additional File 2 for data to Figure 4B. The figure also shows that the variation in the L7 loop lengths is substantial ( $42.9 \pm 14.7$  amino acids), see Figure 4B legend for discussion. Thus, with 95% confidence the longest regular loop is the L3 loop with a

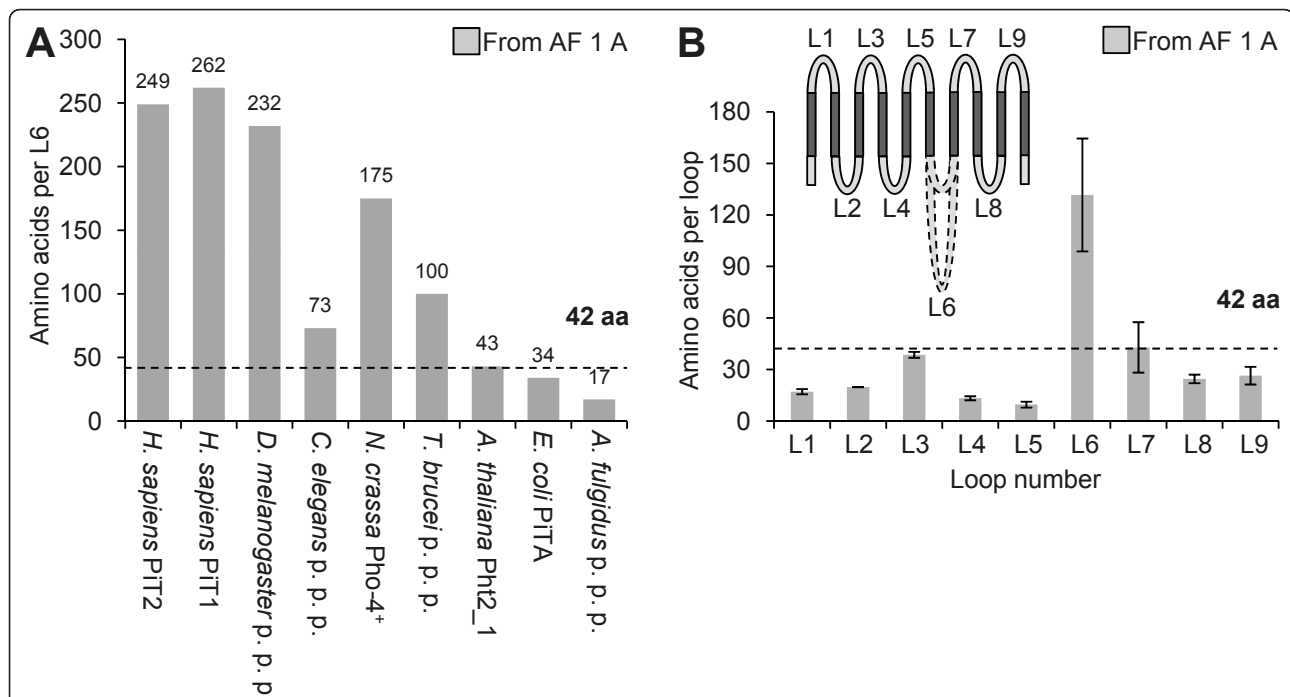


**Figure 4 Investigation of the loop sequence length in PiT family members.** A The amino acid lengths of loop 6 (L6) are plotted for nine PiT family members (*H. sapiens* PiT2, *H. sapiens* PiT1, *N. crassa* Pho-4<sup>+</sup>, *A. thaliana* Pht2\_1, *E. coli* PiTA, and putative phosphate permeases from *D. melanogaster*, *C. elegans*, *T. brucei*, and *A. fulgidus*). The L6 lengths are defined by the predicted TM domains in the protein sequences of the PiT family members; see alignment in and legend to Additional File 1 Figure A (AF 1 A). The maximum limit of a loop length (42 amino acids) estimated in Figure 4B is indicated on the figure. It illustrates that loop lengths at 1 to 42 amino acids define a loop sequence and loop lengths at 43 amino acids or higher defines a domain. B The numbers of amino acids in loop 1 (L1) to loop 9 (L9) in the protein sequences listed in the legend to A are shown. The loop lengths were defined by the sequences connecting the predicted TM domains in the protein sequences for the nine PiT family members; see alignment in and legend to Additional File 1 Figure A (AF 1 A). Data are the mean value of (n) numbers of loops counted  $\pm$ SEM, see Additional File 2 for data. The stippled line indicates the maximum length for a loop sequence (L3) which is  $\sim 42$  amino acids given with 95% confidence ( $38.6 \pm 3.4$  amino acids  $\sim 35$  to 42 amino acids). Note that the 95% confidence interval for L7 is  $42.9 \pm 28.8$  amino acids, illustrating that this loop length is subjected to high uncertainty because of an unusually long L7 in *E. coli* PiTA. The 95% confidence interval for L7 calculated when excluding L7 *E. coli* PiTA is  $28.3 \pm 2.4$  amino acids. The topology model indicates the positions of L1 to L9; stippled loops indicate the observed variable lengths of L6 (the large intracellular domain).

maximum length of 42 amino acids, see legend to Figure 4B for discussion. The definition of the maximum length of a loop also has the impact that the L7 of *E. coli* PiTA consisting of 160 amino acids (Additional File 1 Figure A) has to be considered a domain. In summary, analysis of the sizes of the loop sequences L1 to L9 in nine PiT family members from all kingdoms led to the determination of a limit of maximum 42 amino acids in a regular loop sequence - and sequences longer than 42 amino acids are highly likely domains. In support of our calculations of the maximum loop length for PiT-proteins is a previous study of 243 transmembrane domain-containing sequences, with 146 sequences being multi-transmembrane spanning, showing that ~90% of the loops are shorter than 40 amino acid residues [46]. Another study supporting our finding is the analysis of loops in 79 existing 3D structures of transmembrane proteins showing that the majority of loops connecting transmembrane domains are shorter than 50 amino acid residues [47].

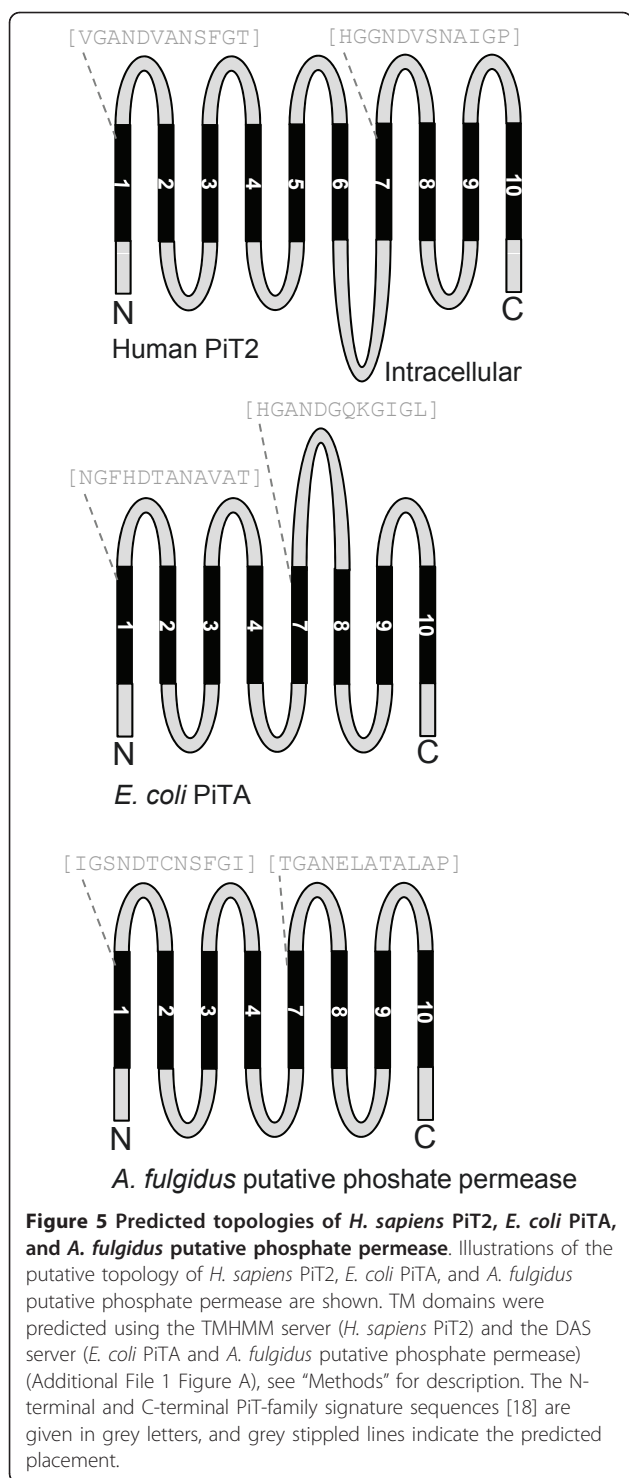
The proteins in Figure 4A with L6 loop sizes smaller than 42 amino acids are the archaeal putative phosphate permease and the bacterial PiTA protein, implying that single cell organisms without nuclei that rarely harbor membrane-bound organelles cope without the large intracellular domain, whereas single cell animals (protozoan's) with nuclei and membrane-bound organelles have distinct L6 domains as shown for the *T. brucei* putative phosphate permease (Figure 4A). Altogether this suggest a role(s) for the large intracellular domain, which is not directly related to  $P_i$  transport *per se*, and it also suggest that the large intracellular domain (L6) may have increased in length during the evolution from archaea to chordata as a consequence of adaptation to more complex environments.

Besides a difference in the lengths of L6, a difference in the number of TM domains in the PiT family members was observed (Additional File 1 Figures A and B). The illustration of TM domain conservedness (black boxes) and TM domains, which are suggested by us to be present but not predicted by protein sequence analysis using the TMHMM server (red boxes, see argumentation in legend to Additional File 1 Figure A), shows the following conservedness of TMs: TM 4, TM 8, TM 10 (fully conserved) > TM 5, TM 6 (fully conserved in eukaryotes) > TM 1, TM 2, TM 3 > TM 9 > TM 7 (least conserved) (Additional File 1 Figure B). The most prominent observation is that *E. coli* PiTA and *A. fulgidus* putative phosphate permease both lack the 5<sup>th</sup> and 6<sup>th</sup> TM domains (Additional File 1 Figures A and B). This in addition to the previous observation that these two proteins also lack the L6 domain (Figure 4A), suggest that the 5<sup>th</sup> and 6<sup>th</sup> TM domains and

the L6 domain are dispensable for  $P_i$  transport function, and that a basic  $P_i$ -transporting unit of the PiT family members can be identified. This unit would consist of regions flanking the large intracellular domain (L6) but highly likely also be devoid of the 5<sup>th</sup> and 6<sup>th</sup> TM domains. Interestingly, in support of this theory, drawing of the putative topology models for human PiT2, *E. coli* PiTA, and *A. fulgidus* putative phosphate permease based on the alignment in Additional File 1 Figure A, shows that the bacterial and archaeal proteins have a predicted eight TM backbone where the N-terminal PiT-family signature sequence is placed in the 1<sup>st</sup> extracellular loop (L1) and the C-terminal PiT family signature sequence is placed in the 3<sup>rd</sup> extracellular loop (L7) (Figure 5). In comparison, the drawing of the putative topology model for human PiT2 shows a backbone of 10 TM domains where the N-terminal and C-terminal PiT-family signature sequences are placed in the 1<sup>st</sup> extracellular loop (L1) and the 4<sup>th</sup> extracellular loop (L7), respectively (Figure 5). An interpretation of these drawings could be that the intraprotein locations of the N-terminal and C-terminal PiT-family signature sequences are of importance, and that TM 1 to TM 4 and TM 7 to TM 10 constitute a core sustaining the  $P_i$ -transporting function whereas TM 5 and TM 6 and the large intracellular domain (L6) constitute a regulatory unit. Finally, the amino acids identified as being critical for  $P_i$  transport function are located in the ProDom domains suggested in 2004 (TM 1 to TM 4 and TM 7 to TM 10) [27] (Figure 1) in agreement with the 5<sup>th</sup> and 6<sup>th</sup> TM domains and the large intracellular domain (L6) might be dispensable for the  $P_i$  transport function.

#### Design of human PiT2 truncation mutants

To identify the minimal  $P_i$ -transporting unit, two human PiT2 truncation mutants were analyzed. They were designed to address the  $P_i$  transport function and the gamma-retroviral receptor functions of: 1) A human PiT2 mutant protein, which consists of the 10 TM domains and a L6 loop of 18 amino acids (human PiT2 P<sub>236</sub>-S<sub>253</sub>) creating the mutant human PiT2 $\Delta$ R<sub>254</sub>-V<sub>483</sub>. The human PiT2 $\Delta$ R<sub>254</sub>-V<sub>483</sub> mutant does not resemble a naturally occurring homolog found in lower species, and it is merely designed to address if the large intracellular domain is dispensable for Na<sup>+</sup>-dependent  $P_i$ -uptake (Figure 1), and 2) A human PiT2 mutant protein that resembles an archaeal and bacterial homolog with respect to protein composition, i.e., lacking the 5<sup>th</sup> and 6<sup>th</sup> TM domains and the large intracellular domain (L<sub>183</sub>-V<sub>483</sub>) (human PiT2 $\Delta$ L<sub>183</sub>-V<sub>483</sub>) (Figure 1). Note that in the Salaün model the 5<sup>th</sup> and 6<sup>th</sup> TM domains correspond to TMVI and TMVII (Figure 2).



**The large intracellular domain (R<sub>254</sub>-V<sub>483</sub>) of human PiT2 is dispensable for P<sub>i</sub> transport function whereas the fragment L<sub>183</sub>-V<sub>483</sub> is more critical for P<sub>i</sub> transport function**

The Na<sup>+</sup>-dependent <sup>32</sup>P<sub>i</sub> transport function of wildtype human PiT2 and the human PiT2-derived truncation

mutants PiT2ΔL<sub>183</sub>-V<sub>483</sub> and PiT2ΔR<sub>254</sub>-V<sub>483</sub> (Figure 1) were analyzed in *X. laevis* oocytes (Figure 6).

Oocytes injected with cRNA encoding human PiT2 supported a <sup>32</sup>P<sub>i</sub> uptake of 79.61 ± 17.74 pmol/oocyte-hour (Figure 6A) and 44.96 ± 0.46 pmol/oocyte-hour (Figure 6B) at pH 7.5 in agreement with previous results [18,28,45].

The <sup>32</sup>P<sub>i</sub> transport activities of the PiT2 mutant lacking the major part of the large intracellular domain, human PiT2ΔR<sub>254</sub>-V<sub>483</sub>, (47.38 ± 6.59 pmol/oocyte-hour (Figure 6A) and 38.74 ± 3.73 pmol/oocyte-hour (Figure 6B)) were indistinguishable from those of PiT2 (*P* = 0.119) (Figure 6A) and *P* = 0.553 (Figure 6B)); see Additional File 2 for data and statistics to Figure 6. Thus, the large intracellular domain of human PiT2 but 18 amino acids (fragment R<sub>254</sub>-V<sub>483</sub>) is dispensable for its P<sub>i</sub> transport function.

The <sup>32</sup>P<sub>i</sub> transport activity of the human PiT2 mutant lacking the large intracellular domain as well as the 5<sup>th</sup> and 6<sup>th</sup> TM domains, PiT2ΔL<sub>183</sub>-V<sub>483</sub> (Figure 1), was severely impaired (3.93 ± 0.44 pmol/oocyte-hour (Figure 6A) and 8.33 ± 2.85 pmol/oocyte-hour (Figure 6B)) when compared to the P<sub>i</sub> transport function of wildtype PiT2

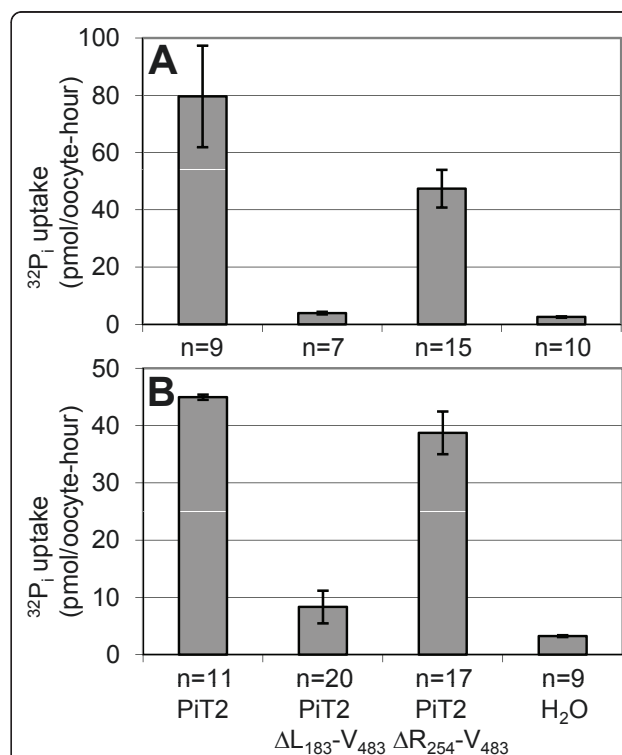


**Figure 6** Na<sup>32</sup>P<sub>i</sub> uptake mediated by human PiT2 and truncation mutants analyzed in *X. laevis* oocytes. Oocytes were injected with H<sub>2</sub>O or cRNA of the indicated constructs. Two (experiment A) or three (experiment B) days later, a <sup>32</sup>P<sub>i</sub> uptake assay was performed and the <sup>32</sup>P<sub>i</sub> uptake in individual oocytes was measured. Data are the mean value of (n) numbers of oocytes ± SEM, see Additional File 2 for data and statistics.

( $P = 0.003$  (Figure 6A) and  $P = 0.004$  (Figure 6B)). However, interestingly the mutant did support low levels of  $P_i$  uptake significantly different from  $H_2O$ -injected oocytes ( $2.56 \pm 0.24$  pmol/oocyte-hour (Figure 6A) and  $3.24 \pm 0.17$  pmol/oocyte-hour (Figure 6B)) ( $P = 0.011$  (Figure 6A) and  $P = 0.008$  (Figure 6B)).

#### Viral receptor function of mutant PiT2 proteins

Using the transient transfection-infection assay, we analyzed whether the deletions in human PiT2 affected their viral receptor functions for A-MLV and 10A1 MLV. Eukaryotic expression plasmids encoding human PiT2 and the mutant proteins were transfected into CHO K1 cells. As expected, human PiT2 transfected cells were permissive for infection by both 10A1 MLV and A-MLV vector pseudotypes (Table 1). While the human PiT2 truncation mutant lacking the large intracellular domain, human PiT2 $\Delta R_{254-483}$  (Figure 1) was a fully functional  $P_i$  transporter (Figure 6), it only supported low levels of PiT2 cognate gamma-retroviral infection (Table 1). Note that human PiT2 $\Delta R_{254-483}$  was tested once for A-MLV receptor function and twice for 10A1 MLV receptor function. The A-MLV study was done in parallel to a 10A1 MLV receptor function study using the same set of plasmid precipitates. Interestingly, the human PiT2 truncation mutant lacking the 5<sup>th</sup> and 6<sup>th</sup> TM domains in addition to the large intracellular domain, human PiT2 $\Delta L_{183-483}$  (Figure 1), supported substantial levels of PiT2 cognate gamma-retroviral infection (Table 1) [31] showing that its low levels of  $P_i$  transport function were not due to incorrect processing of this mutant to the cell surface.

PiT2 regions directly involved in receptor function for 10A1 MLV and A-MLV have also been identified by expression of chimeric proteins in CHO K1 cells and were found to be located in the putative extracellular

loops 2 (L3) and 4 (L7) (Figure 1) [26,37,48,49]. Both of the human PiT2 mutants, PiT2 $\Delta R_{254-483}$  and PiT2 $\Delta L_{183-483}$ , harbor extracellular loops 2 (L3) and 4 (L7) according to the Johann PiT2 model (Figure 1). Based on their - here identified -  $P_i$  transport abilities, it is unlikely that PiT2 $\Delta R_{254-483}$  is less expressed at the cell surface than PiT2 $\Delta L_{183-483}$ , and the observation that the less truncated human PiT2 mutant protein is a worse gamma-retroviral receptor than a more heavily truncated human PiT2 mutant protein might instead reflect a disturbance of the folding and/or conformation of the extracellular loops 2 (L3) and 4 (L7) due to the sole presence of the extracellular loop 3 (L5) without the large intracellular domain in PiT2 $\Delta R_{254-483}$ .

#### Intron-exon borders of the human PiT genes *SLC20A1* and *SLC20A2*

The human PiT proteins are encoded by genes that localize to different chromosomes. The human gene, *SLC20A1*, encoding the PiT1 protein is located on chromosome 2 at position q13 [50,51], and the human gene, *SLC20A2*, encoding the PiT2 protein is located on chromosome 8 at position p11.2 [8,52,53].

To analyze the gene structure of *SLC20A1* and *SLC20A2*, the intron-exon borders in each of the genes were determined using the SPIDEY mRNA-to-genome DNA alignment as described in "Methods". The intron-exon borders are marked with stars (☆) and vertical lines in the PiT1 and PiT2 protein sequences in the alignment of nine PiT family members in Additional File 1 Figure A.

Eight out of nine intron-exon borders (labeled ☆ a to e and ☆ g to i on PiT1 and PiT2 in Additional File 1 Figure A) in *SLC20A1* and *SLC20A2* are predicted to be homologous. One intron-exon border (labeled ☆ f<sup>1</sup> (*SLC20A2*) and f<sup>2</sup> (*SLC20A1*)) are displaced giving a gap

**Table 1 Levels of 10A1 MLV and A-MLV entry supported by human PiT2 and derived truncation mutants<sup>a</sup>**

| Construct <sup>b</sup>    | No. (%) of cells infected <sup>c</sup> |                     |          |                     |                     |                     |          |         |
|---------------------------|--|---------------------|----------|---------------------|---------------------|---------------------|----------|---------|
|                           | A-MLV                                  |                     |          | 10A1 MLV            |                     |                     |          |         |
|                           | Expt 1 <sup>d</sup>                    | Expt 2 <sup>d</sup> | Expt 4   | Expt 1 <sup>d</sup> | Expt 2 <sup>d</sup> | Expt 3 <sup>d</sup> | Expt 4   | Expt 5  |
| PiT2 (pOJ74)              | 100 ± 22                               | 100 ± 8             | 100 ± 12 | 100 ± 5             | 100 ± 8             | 100 ± 9             | 100 ± 11 | 100 ± 9 |
| PiT2 $\Delta L_{183-483}$ | 25 ± 1                                 | 13 ± 2              | ND       | 10 ± 1              | 12 ± 4              | 24 ± 3              | ND       | 25 ± 3  |
| PiT2 $\Delta R_{254-483}$ | ND <sup>e</sup>                        | ND                  | 4 ± >1   | ND                  | ND                  | ND                  | 1 ± >1   | 1 ± >1  |
| Empty vector <sup>f</sup> | <0.0008                                | <0.002              | <0.01    | <0.002              | <0.001              | <0.001              | <0.007   | <0.003  |

<sup>a</sup>The experimental setup is described in the text. A-MLV and 10A1 MLV vector pseudotypes were tested on the same precipitates made from CsCl-purified plasmids in experiment 4. In experiment 5, Qiagen maxiprep-purified plasmids were used for preparing precipitates and only the 10A1 MLV vector pseudotype was tested.

<sup>b</sup>Receptor and mutant receptor sequences were cloned into pcDNA1A<sup>+</sup>tkpA.

<sup>c</sup>The data are averages of three independent transfections ± SEM. The average number of blue cells per three 60-mm-diameter dishes transfected with a plasmid encoding PiT2 was assigned a value of 100% (57,000, 90,000, and 32,000 blue cells per dish for A-MLV in experiment 4 and for 10A1 MLV in experiments 4 and 5, respectively).

<sup>d</sup>Data are from Böttger and Pedersen 2004 [31]; please see article for details.

<sup>e</sup>ND, not determined.

<sup>f</sup>Values are based on the detection limit of 1 blue cell per three 60-mm-diameter dishes.

corresponding to 12 amino acids (~36 nucleotides). These two borders are placed in the middle of the genome sequences, which encode the large intracellular domain (L6) of the human PiT proteins. As seen from Additional File 1 Figure A, the alignment between the human PiT proteins in this region is poor and the gap highly likely reflects this, and not a significant difference in intron-exon structure between *SLC20A1* and *SLC20A2*.

Interestingly, in support of the theory that the 5<sup>th</sup> and 6<sup>th</sup> TM domains can be dispensable for P<sub>i</sub> transport function, is the observation that these TM domains are encoded by two different exons, see Additional File 1 Figure A (☆ labeled c to d, and ☆ labeled d to e), and therefore the possibility exists that the sequences in these two exons have entered later in evolution.

### Specialized functions of the mammalian PiT proteins

Mammalian PiT proteins are expressed in all tissues investigated and due to their broad expression profiles, they have been suggested to accommodate house-keeping functions, i.e., supplying cells with P<sub>i</sub> to maintain basic cellular functions [2,20,54]. However, in recent years additional specialized functions of the PiT proteins have been reported. These include roles for PiT2 in proximal tubule phosphate reabsorption [55], and for PiT1 in regulation of parathyroid gland PTH production [56,57], cell proliferation [29,58,59], and in tumor necrosis factor (TNF) induced apoptosis [60]. Recent studies also indicate that both the PiT proteins function as P<sub>i</sub> sensors [27,56], reviewed in [61]. Interestingly, some of these functions, that is, PiT2's suggested role in P<sub>i</sub> sensing [27] and PiT1's role in cell proliferation and TNF-induced apoptosis [29,59,60] have been shown to be independent of the P<sub>i</sub> transport functions of the proteins.

PiT1 has also been implicated in normal chondroblastic and osteoblastic differentiation and mineralization processes [62-66], as well as trans-differentiation of vascular smooth muscle cells to cells with characteristics of chondro-/osteoblasts in the pathologic process of vascular calcification at hyperphosphatemia [67]. More rodent *in vivo* models have been used to study the role of PiT1 in normal bone formation and/or embryonic development. Rats with transgenic overexpression of PiT1 showed no major bone deformity during skeletal development [57]. However, these rats displayed a slight but significant decrease in the bone mineral content of the whole skeleton together with a reduction albeit non-significant in the total bone area [57]. The role of PiT1 during embryonic mouse development has been studied by two different groups employing early conditional excision of *SLC20A1* Exons 3-4 [68] and *SLC20A1* Exon 5 [59], which resulted in homozygous embryonic

lethality. Both studies find that the embryos are anemic and do not survive past E12.5, at which stage the morphology shows reduced growth [59,68]; the anemia was found to be due to severe defects in liver development [59]. Comparison of wildtype mice to mice with low (15%) expression of PiT1 mRNA showed that some of the latter mice displayed impaired bone mineralization at birth, while 15-days old mice showed no major differences in mineralization [59]. Interestingly, in embryos (E11.5) lacking PiT1 expression Beck and coworkers found an upregulated PiT2 expression, which however could not rescue the embryos past E12.5, and the authors therefore suggest that the critical non-redundant role of PiT1 in development is not P<sub>i</sub>-uptake [59]. Altogether, the *in vivo* studies do not exclude a role for PiT1 in normal bone formation, although they imply that PiT1 is not critical for the early skeletal developmental processes.

The alignment and analyses of exon structure together with the observed P<sub>i</sub> transport functions of the PiT2 deletion mutants presented here might suggest that the regions of the PiT proteins involved in the P<sub>i</sub>-transport independent functions map to sequences in the 5<sup>th</sup> and 6<sup>th</sup> TM domains and/or in the large intracellular domain. In line with this, we are currently investigating the function of the large intracellular domain of the human PiT2 protein and our results support the hypothesis that the large intracellular domain has other functions than P<sub>i</sub> transport.

### Conclusions

Investigation of the P<sub>i</sub> transport and retroviral receptor functions of the human PiT proteins has allowed for identification of a histidine residue (human PiT2 H<sub>502</sub>) in the C-terminal PiT family signature sequence as being critically involved in P<sub>i</sub> transport function. Moreover, we show that a PiT1 glutamate residue (human PiT1 E<sub>70</sub>) positioned in the 2<sup>nd</sup> TM domain is critical for P<sub>i</sub> transport function in agreement with the former identification of the equivalent glutamate in human PiT2 (human PiT2 E<sub>55</sub>) as being critical for P<sub>i</sub> transport function [28].

We have shown that a human PiT2 mutant consisting of the 10 TM domains and minor loops (human PiT2ΔR<sub>254</sub>-V<sub>483</sub>) transports P<sub>i</sub> as wildtype PiT2, proving that the large intracellular domain (L6) is dispensable for P<sub>i</sub> transport function. A further truncated human PiT2 mutant consisting of the 1<sup>st</sup> to 4<sup>th</sup> TM domains linked to the 7<sup>th</sup> to 10<sup>th</sup> TM domains and the minor loop sequences connecting the TMs (human PiT2ΔL<sub>183</sub>-V<sub>483</sub>), and which resembles archaeal and bacterial homologs, sustained low levels of P<sub>i</sub> transport. This protein harbors the ProDom domains defining the PiT family members and, moreover, harbors all the amino

acids so far identified as being critical for  $P_i$  transport function.

The above results showing that truncated human PiT2 mutant proteins - one of which resembles a phosphate permease from bacteria and a putative phosphate permease from archaea - support  $P_i$  transport, point to the conclusion that the overall structure of the PiT family proteins has remained unchanged during evolution and that a basic  $P_i$ -transporting unit exists.

## Additional material

### Additional file 1: Protein sequence alignment of nine PIT family members from all kingdoms.

A The 10 putative TM domains according to the Johann topology model are shown on the human PiT2 sequence using black boxes with white filling [8,20]; the putative large intracellular domain (L6) of human PiT2, according to this model, spans the amino acid sequence: P<sub>236</sub>-V<sub>483</sub>. The N-terminal and C-terminal PIT family signature sequences [18] are shown on the alignment in black boxes with grey filling. Human PiT1 E<sub>70</sub> in the 2<sup>nd</sup> TM domain and human PiT2 H<sub>502</sub> in the 7<sup>th</sup> TM domain are indicated with circles. The TMHMM-predicted TM domains of the eukaryotic protein sequences for PiT family members and the DAS-predicted TM domains of the prokaryotic protein sequences for PiT family members are shown in black bold. The red bold sequences represent TM-domains, which we suggest exist, however, they were not predicted by the servers: *N. crassa* Pho-4<sup>+</sup> TM 1 (sequence Q<sub>5</sub>-L<sub>24</sub>) is suggested to be homologous to the TM 1 predicted in the *C. elegans* putative phosphate permease protein sequence. The presence of Pho-4<sup>+</sup> TM 1 is also based on the assumption that the N-terminal PiT-family signature sequences should be placed equivalently (extracellularly in L1) in all PiT family members. *A. thaliana* Pht2\_1 TM 2 (sequence A<sub>187</sub>-G<sub>211</sub>) is suggested to be homologous to the TM 2 predicted in the *T. brucei* putative phosphate permease protein sequence. The presence of Pht2\_1 TM 2 is also based on experimental assignment of the L6 for rat PiT2 to the cytoplasmic space [21], and Pht2\_1 therefore requires a TM 2 to fulfill this criteria. *H. sapiens* PiT2 TM 3 (sequence T<sub>83</sub>-A<sub>105</sub>) is suggested to be homologous to the TM 3 predicted in the *H. sapiens* PiT1 protein sequence. Investigation of a human PiT1/PiT2 chimera where the PiT1 backbone harbors the human PiT2 sequence G<sub>120</sub>-V<sub>141</sub> showed that this sequence conferred A-MLV receptor function upon human PiT1 [48], and the G<sub>120</sub>-V<sub>141</sub> sequence is therefore highly likely extracellular in both human PiT paralogs and this requires the presence of TM 3 in human PiT2. TM 7 domains in putative phosphate permeases from *C. elegans* (sequence Q<sub>330</sub>-A<sub>349</sub>), *D. melanogaster* (sequence M<sub>472</sub>-G<sub>491</sub>), *T. brucei* (sequence Y<sub>346</sub>-A<sub>365</sub>), and *N. crassa* Pho-4<sup>+</sup> (sequence Y<sub>318</sub>-A<sub>337</sub>) are suggested to be homologous to the TM 7 predicted in *H. sapiens* PiT2 and PiT1 sequences. The presence of TM 7 in putative phosphate permeases from *C. elegans*, *D. melanogaster*, *T. brucei*, and *N. crassa* Pho-4<sup>+</sup> is also based on the assumption that the C-terminal PiT-family signature sequences should be placed equivalently (extracellularly in L7) in all PiT family members. Moreover, investigation of a Pho-4<sup>+</sup>/human PiT2 chimera where the Pho-4<sup>+</sup> backbone harbors the human PiT2 sequences C<sub>117</sub>-I<sub>143</sub> (stretch in L3) and L<sub>512</sub>-A<sub>531</sub> (stretch in L7) showed that these sequences confer A-MLV receptor function upon Pho-4<sup>+</sup>[26], and these sequences are therefore highly likely extracellular and this requires the presence of a TM 7. Similarly, investigation of a Pho-4<sup>+</sup>/human PiT1 chimera where the Pho-4<sup>+</sup> backbone harbors the human PiT1 sequence L<sub>545</sub>-S<sub>556</sub> (stretch in L7) showed that these sequences confer GALV receptor function upon Pho-4<sup>+</sup>[25]. *H. sapiens* PiT2 TM 9 (sequence G<sub>571</sub>-S<sub>593</sub>) and *H. sapiens* PiT1 TM 9 (sequence G<sub>599</sub>-S<sub>521</sub>) are suggested to be homologous to the TM 9 predicted in RPHO-1 *R. norvegicus* (human PiT1 ortholog) protein sequence G<sub>601</sub>-S<sub>623</sub> [Swiss-Prot: Q9JJPO] using the TMHMM server (data not shown). *N. crassa* Pho-4<sup>+</sup> TM 9 (sequence L<sub>523</sub>-G<sub>545</sub>) is suggested to be homologous to the TM 9 predicted in *C. elegans* putative phosphate permease protein sequence. The TM 9 is required to orient the TM 10 equivalently in all PiT family members. Lower case letters represent TMHMM- or DAS-predicted TM

sequences, which we based on either too small length to comprise a TM or due to suggested extracellular position (see above) found were non-compatible with regular TM domains; however, these sequences might instead "dip" into the membrane lipid bilayer. It should be noted that these sequences are counted as being part of the loop sequences in Figure 4. A star (☆) (labeled a to i) and a vertical line indicate the position of an intron-exon border in each of the human PiT genes determined by use of the SPIDEY mRNA-to-genome DNA alignment as described in "Methods". Below the alignment, the names, species, phylas, kingdoms, Swiss-Prot accession numbers, and the amino acid lengths of the nine proteins are given. B The server-predicted TM domains (black boxes) and the by us suggested TM domains (red boxes) for each of the nine PiT family members are depicted in order to illustrate the conservedness of the TM domains: TM 4, TM 8, TM 10 (fully conserved) > TM 5, TM 6 (fully conserved in eukaryotes) > TM 1, TM 2, TM 3 > TM 9 > TM 7 (least conserved). The white asterisk indicates a prediction of a unique TM domain in the unusually long N-terminal sequence of *A. thaliana* Pht2\_1.

**Additional File 2: Data and statistics.** Average <sup>32</sup>P<sub>i</sub> uptakes in oocytes given as pmol/oocyte-hour ±SEM, information regarding the number (n) of oocytes measured, and the statistics (P values) for Figures 3A-B and Figure 6 are available in Additional File 2. Average numbers of blue (infected) cells per dish from three dishes ±SEM and the statistics (P values) for Figures 3C-E are available in Additional File 2. Average loop lengths given as amino acids ±SEM and information regarding the number (n) of loops counted for Figure 4B are available in Additional File 2.

### List of abbreviations used

10A1 MLV: retrovirus closely related to A-MLV, A-MLV: amphotropic murine leukemia virus, CHO K1: Chinese hamster ovary K1, GALV: gibbon ape leukemia virus, FeLV-B: feline leukemia virus subgroup B, P<sub>i</sub>: inorganic phosphate, PiT: P<sub>i</sub> transporter, TM: transmembrane.

### Acknowledgements and Funding

We thank Drs. Bryan O'Hara for pOJ74 and pOJ75, Maribeth V. Eiden for the PA317GBN and PG13GBN cell lines, Joyce Dunn for the FeLV-B virus stock, and Jan Egebjerg Jensen for use of his *X. laevis* oocyte facilities. We furthermore thank Bente Andersen for excellent technical assistance. This work was supported by the Lundbeck Foundation (Grant number 14/02), the Novo Nordisk Foundation, the Danish Medical Research Foundation (Grant numbers (09-058816) 22-03-0254, 09-061652 (271-06-0564), 09-063569 (271-07-0598), 09-066064 (271-08-1005), an Engineer Arne Hansen grant, and the Intramural Budget at the Institute of Clinical Medicine at Aarhus University.

### Author details

<sup>1</sup>Department of Molecular Biology, Aarhus University, C. F. Møllers Allé 3, Aarhus C, DK-8000, Denmark. <sup>2</sup>Institute of Clinical Medicine, Aarhus University, Brendstrupgårdsvej 100, Aarhus N, DK-8200, Denmark. <sup>3</sup>Department of Haematology, Aarhus University Hospital, Tage-Hansens gade 2, DK-8000 Aarhus C, Denmark. <sup>4</sup>Department of Medical Biochemistry, Ole Worms Allé 3, Aarhus University, DK-8000 Aarhus C, Denmark.

### Authors' contributions

PB and LP conceived the study and designed the experiments. PB did the experimental work, and drafted the manuscript. PB and LP edited and approved the final version of the manuscript.

Received: 7 January 2011 Accepted: 17 May 2011

Published: 17 May 2011

### References

- Oláh Z, Lehel C, Anderson WB, Eiden MV, Wilson CA: **The cellular receptor for gibbon ape leukemia virus is a novel high affinity sodium-dependent phosphate transporter.** *J Biol Chem* 1994, **269**(41):25426-25431.
- Kavanaugh MP, Miller DG, Zhang W, Law W, Kozak SL, Kabat D, Miller AD: **Cell-surface receptors for gibbon ape leukemia virus and amphotropic**

- murine retrovirus are inducible sodium-dependent phosphate symporters. *Proc Natl Acad Sci USA* 1994, **91**(15):7071-7075.
3. Kavanaugh MP, Kabat D: Identification and characterization of a widely expressed phosphate transporter/retrovirus receptor family. *Kidney Int* 1996, **49**(4):959-963.
  4. Virkki LV, Biber J, Murer H, Forster IC: Phosphate transporters: a tale of two solute carrier families. *Am J Physiol Renal Physiol* 2007, **293**(3):F643-654.
  5. Wain HM, Bruford EA, Lovering RC, Lush MJ, Wright MW, Povey S: Guidelines for human gene nomenclature. *Genomics* 2002, **79**(4):464-470.
  6. Saier MH Jr: A functional-phylogenetic classification system for transmembrane solute transporters. *Microbiol Mol Biol Rev* 2000, **64**(2):354-411.
  7. O'Hara B, Johann SV, Klinger HP, Blair DG, Rubinson H, Dunn KJ, Sass P, Vitek SM, Robins T: Characterization of a human gene conferring sensitivity to infection by gibbon ape leukemia virus. *Cell Growth Differ* 1990, **1**(3):119-127.
  8. van Zeijl M, Johann SV, Closs E, Cunningham J, Eddy R, Shows TB, O'Hara B: A human amphotropic retrovirus receptor is a second member of the gibbon ape leukemia virus receptor family. *Proc Natl Acad Sci USA* 1994, **91**(3):1168-1172.
  9. Miller DG, Edwards RH, Miller AD: Cloning of the cellular receptor for amphotropic murine retroviruses reveals homology to that for gibbon ape leukemia virus. *Proc Natl Acad Sci USA* 1994, **91**(1):78-82.
  10. Miller DG, Miller AD: A family of retroviruses that utilize related phosphate transporters for cell entry. *J Virol* 1994, **68**(12):8270-8276.
  11. Takeuchi Y, Vile RG, Simpson G, O'Hara B, Collins MK, Weiss RA: Feline leukemia virus subgroup B uses the same cell surface receptor as gibbon ape leukemia virus. *J Virol* 1992, **66**(2):1219-1222.
  12. Wilson CA, Farrell KB, Eiden MV: Properties of a unique form of the murine amphotropic leukemia virus receptor expressed on hamster cells. *J Virol* 1994, **68**(12):7697-7703.
  13. Tailor CS, Takeuchi Y, O'Hara B, Johann SV, Weiss RA, Collins MK: Mutation of amino acids within the gibbon ape leukemia virus (GALV) receptor differentially affects feline leukemia virus subgroup B, simian sarcoma-associated virus, and GALV infections. *J Virol* 1993, **67**(11):6737-6741.
  14. Mann BJ, Bowman BJ, Grotelueschen J, Metzberg RL: Nucleotide sequence of pho-4+, encoding a phosphate-repressible phosphate permease of *Neurospora crassa*. *Gene* 1989, **83**(2):281-289.
  15. Martinez P, Persson BL: Identification, cloning and characterization of a derepressible Na<sup>+</sup>-coupled phosphate transporter in *Saccharomyces cerevisiae*. *Mol Gen Genet* 1998, **258**(6):628-638.
  16. Harris RM, Webb DC, Howitt SM, Cox GB: Characterization of PitA and PitB from *Escherichia coli*. *J Bacteriol* 2001, **183**(17):5008-5014.
  17. Daram P, Brunner S, Rausch C, Steiner C, Amrhein N, Bucher M: Pht2;1 encodes a low-affinity phosphate transporter from *Arabidopsis*. *Plant Cell* 1999, **11**(11):2153-2166.
  18. Bøttger P, Pedersen L: Evolutionary and experimental analyses of inorganic phosphate transporter PIT family reveals two related signature sequences harboring highly conserved aspartic acids critical for sodium-dependent phosphate transport function of human Pit2. *FEBS J* 2005, **272**(12):3060-3074.
  19. Werner A, Kinne RK: Evolution of the Na-P(i) cotransport systems. *Am J Physiol Regul Integr Comp Physiol* 2001, **280**(2):R301-312.
  20. Johann SV, Gibbons JJ, O'Hara B: GLVR1, a receptor for gibbon ape leukemia virus, is homologous to a phosphate permease of *Neurospora crassa* and is expressed at high levels in the brain and thymus. *J Virol* 1992, **66**(3):1635-1640.
  21. Chien ML, Foster JL, Douglas JL, Garcia JV: The amphotropic murine leukemia virus receptor gene encodes a 71-kilodalton protein that is induced by phosphate depletion. *J Virol* 1997, **71**(6):4564-4570.
  22. Farrell KB, Russ JL, Murthy RK, Eiden MV: Reassessing the role of region A in Pit1-mediated viral entry. *J Virol* 2002, **76**(15):7683-7693.
  23. Farrell KB, Tusnady GE, Eiden MV: New structural arrangement of the extracellular regions of the phosphate transporter SLC20A1, the receptor for gibbon ape leukemia virus. *J Biol Chem* 2009, **284**(43):29979-29987.
  24. Salaün C, Rodrigues P, Heard JM: Transmembrane topology of Pit-2, a phosphate transporter-retrovirus receptor. *J Virol* 2001, **75**(12):5584-5592.
  25. Pedersen L, van Zeijl M, Johann SV, O'Hara B: Fungal phosphate transporter serves as a receptor backbone for gibbon ape leukemia virus. *J Virol* 1997, **71**(10):7619-7622.
  26. Lundorf MD, Pedersen FS, O'Hara B, Pedersen L: Amphotropic murine leukemia virus entry is determined by specific combinations of residues from receptor loops 2 and 4. *J Virol* 1999, **73**(4):3169-3175.
  27. Salaün C, Maréchal V, Heard JM: Transport-deficient Pit2 phosphate transporters still modify cell surface oligomers structure in response to inorganic phosphate. *J Mol Biol* 2004, **340**(1):39-47.
  28. Bøttger P, Pedersen L: Two highly conserved glutamate residues critical for type III sodium-dependent phosphate transport revealed by uncoupling transport function from retroviral receptor function. *J Biol Chem* 2002, **277**(45):42741-42747.
  29. Beck L, Leroy C, Salaün C, Margall-Ducos G, Desdouets C, Friedlander G: Identification of a novel function of Pit1 critical for cell proliferation and independent of its phosphate transport activity. *J Biol Chem* 2009, **284**(45):31363-31374.
  30. Saier MH Jr: Eukaryotic transmembrane solute transport systems. *Int Rev Cytol* 1999, **190**:61-136.
  31. Bøttger P, Pedersen L: The central half of Pit2 is not required for its function as a retroviral receptor. *J Virol* 2004, **78**(17):9564-9567.
  32. Higgins DG: CLUSTAL V: multiple alignment of DNA and protein sequences. *Methods Mol Biol* 1994, **25**:307-318.
  33. Sonnhammer EL, von Heijne G, Krogh A: A hidden Markov model for predicting transmembrane helices in protein sequences. *Proc Int Conf Intell Syst Mol Biol* 1998, **6**:175-182.
  34. Cserzo M, Wallin E, Simon I, von Heijne G, Elofsson A: Prediction of transmembrane alpha-helices in prokaryotic membrane proteins: the dense alignment surface method. *Protein Eng* 1997, **10**(6):673-676.
  35. Acquisti C, Kleffe J, Collins S: Oxygen content of transmembrane proteins over macroevolutionary time scales. *Nature* 2007, **445**(7123):47-52.
  36. Wheelan SJ, Church DM, Ostell JM: Spidey: a tool for mRNA-to-genomic alignments. *Genome Res* 2001, **11**(11):1952-1957.
  37. Pedersen L, Johann SV, van Zeijl M, Pedersen FS, O'Hara B: Chimeras of receptors for gibbon ape leukemia virus/feline leukemia virus B and amphotropic murine leukemia virus reveal different modes of receptor recognition by retrovirus. *J Virol* 1995, **69**(4):2401-2405.
  38. Maniatis S, Sambrook J, Fritsch: *Molecular Cloning, A Laboratory Manual*. Cold Spring Harbor Laboratory Press; 3 1989.
  39. McLachlin JR, Mittereder N, Daucher MB, Kadan M, Eglitis MA: Factors affecting retroviral vector function and structural integrity. *Virology* 1993, **195**(1):1-5.
  40. Miller AD, Chen F: Retrovirus packaging cells based on 10A1 murine leukemia virus for production of vectors that use multiple receptors for cell entry. *J Virol* 1996, **70**(8):5564-5571.
  41. Miller AD, Buttimore C: Redesign of retrovirus packaging cell lines to avoid recombination leading to helper virus production. *Mol Cell Biol* 1986, **6**(8):2895-2902.
  42. Miller AD, Garcia JV, von Suhr N, Lynch CM, Wilson C, Eiden MV: Construction and properties of retrovirus packaging cells based on gibbon ape leukemia virus. *J Virol* 1991, **65**(5):2220-2224.
  43. Dreyer K, Pedersen FS, Pedersen L: A 13-amino-acid Pit1-specific loop 4 sequence confers feline leukemia virus subgroup B receptor function upon Pit2. *J Virol* 2000, **74**(6):2926-2929.
  44. Godfrey EW, Sanders GE: Effect of water hardness on oocyte quality and embryo development in the African clawed frog (*Xenopus laevis*). *Comp Med* 2004, **54**(2):170-175.
  45. Bøttger P, Hede SE, Grunnet M, Høyer B, Klærke DA, Pedersen L: Characterization of transport mechanisms and determinants critical for Na<sup>+</sup>-dependent Pi symport of the Pit family paralogs human Pit1 and Pit2. *Am J Physiol Cell Physiol* 2006, **291**(6):C1377-C1387.
  46. Kabsay RY, Gao G, Liao L: An improved hidden Markov model for transmembrane protein detection and topology prediction and its applications to complete genomes. *Bioinformatics* 2005, **21**(9):1853-1858.
  47. Viklund H, Granseth E, Elofsson A: Structural classification and prediction of reentrant regions in alpha-helical transmembrane proteins: application to complete genomes. *J Mol Biol* 2006, **361**(3):591-603.
  48. Leverett BD, Farrell KB, Eiden MV, Wilson CA: Entry of amphotropic murine leukemia virus is influenced by residues in the putative second extracellular domain of its receptor, Pit2. *J Virol* 1998, **72**(6):4956-4961.
  49. Lundorf MD, Pedersen FS, O'Hara B, Pedersen L: Single amino acid insertion in loop 4 confers amphotropic murine leukemia virus receptor function upon murine Pit1. *J Virol* 1998, **72**(5):4524-4527.

50. Kaelbling M, Eddy R, Shows TB, Copeland NG, Gilbert DJ, Jenkins NA, Klinger HP, O'Hara B: **Localization of the human gene allowing infection by gibbon ape leukemia virus to human chromosome region 2q11-q14 and to the homologous region on mouse chromosome 2.** *J Virol* 1991, **65**(4):1743-1747.
51. Palmer G, Manen D, Bonjour JP, Caverzasio J: **Characterization of the human Glvr-1 phosphate transporter/retrovirus receptor gene and promoter region.** *Gene* 1999, **226**(1):25-33.
52. Chien ML, O'Neill E, Garcia JV: **Phosphate depletion enhances the stability of the amphotropic murine leukemia virus receptor mRNA.** *Virology* 1998, **240**(1):109-117.
53. Garcia JV, Jones C, Miller AD: **Localization of the amphotropic murine leukemia virus receptor gene to the pericentromeric region of human chromosome 8.** *J Virol* 1991, **65**(11):6316-6319.
54. Uckert W, Willimsky G, Pedersen FS, Blankenstein T, Pedersen L: **RNA levels of human retrovirus receptors Pit1 and Pit2 do not correlate with infectibility by three retroviral vector pseudotypes.** *Hum Gene Ther* 1998, **9**(17):2619-2627.
55. Villa-Belosta R, Ravera S, Sorribas V, Stange G, Levi M, Murer H, Biber J, Forster IC: **The Na<sup>+</sup>-Pi cotransporter Pit-2 (SLC20A2) is expressed in the apical membrane of rat renal proximal tubules and regulated by dietary Pi.** *Am J Physiol Renal Physiol* 2009, **296**(4):F691-699.
56. Miyamoto K, Ito M, Segawa H, Kuwahata M: **Secondary hyperparathyroidism and phosphate sensing in parathyroid glands.** *J Med Invest* 2000, **47**(3-4):118-122.
57. Suzuki A, Ammann P, Nishiwaki-Yasuda K, Sekiguchi S, Asano S, Nagao S, Kaneko R, Hirabayashi M, Oiso Y, Itoh M, Caverzasio J: **Effects of transgenic Pit-1 overexpression on calcium phosphate and bone metabolism.** *J Bone Miner Metab* 2010, **28**(2):139-148.
58. Kimata M, Michigami T, Tachikawa K, Okada T, Koshimizu T, Yamazaki M, Kogo M, Ozono K: **Signaling of extracellular inorganic phosphate up-regulates cyclin D1 expression in proliferating chondrocytes via the Na<sup>+</sup>/Pi cotransporter Pit-1 and Raf/MEK/ERK pathway.** *Bone* 2010, **47**(5):938-947.
59. Beck L, Leroy C, Beck-Cormier S, Forand A, Salaun C, Paris N, Bernier A, Urena-Torres P, Prie D, Ollero M, Coulombel L, Friedlander G: **The phosphate transporter Pit1 (Slc20a1) revealed as a new essential gene for mouse liver development.** *PLoS One* 2010, **5**(2):e9148.
60. Salaun C, Leroy C, Rousseau A, Boitez V, Beck L, Friedlander G: **Identification of a novel transport-independent function of PIT1/SLC20A1 in the regulation of TNF-induced apoptosis.** *J Biol Chem* 2010, **285**(45):34408-34418.
61. Khoshniat S, Bourguin A, Julien M, Weiss P, Guicheux J, Beck L: **The emergence of phosphate as a specific signaling molecule in bone and other cell types in mammals.** *Cell Mol Life Sci* 2011, **68**(2):205-218.
62. Nielsen LB, Pedersen FS, Pedersen L: **Expression of type III sodium-dependent phosphate transporters/retroviral receptors mRNAs during osteoblast differentiation.** *Bone* 2001, **28**(2):160-166.
63. Palmer G, Zhao J, Bonjour J, Hofstetter W, Caverzasio J: **In vivo expression of transcripts encoding the Glvr-1 phosphate transporter/retrovirus receptor during bone development.** *Bone* 1999, **24**(1):1-7.
64. Suzuki A, Ghayor C, Guicheux J, Magne D, Quillard S, Kakita A, Ono Y, Miura Y, Oiso Y, Itoh M, Caverzasio J: **Enhanced Expression of the Inorganic Phosphate Transporter Pit-1 Is Involved in BMP-2-Induced Matrix Mineralization in Osteoblast-Like Cells.** *J Bone Miner Res* 2006, **21**(5):674-683.
65. Sugita A, Kawai S, Hayashibara T, Amano A, Ooshima T, Michigami T, Yoshikawa H, Yoneda T: **Cellular ATP synthesis mediated by type III sodium-dependent phosphate transporter Pit-1 is critical to chondrogenesis.** *J Biol Chem* 2011, **286**(4):3094-3103.
66. Yoshiko Y, Candelieri GA, Maeda N, Aubin JE: **Osteoblast autonomous Pi regulation via Pit1 plays a role in bone mineralization.** *Mol Cell Biol* 2007, **27**(12):4465-4474.
67. Li X, Yang HY, Giachelli CM: **Role of the sodium-dependent phosphate cotransporter, Pit-1, in vascular smooth muscle cell calcification.** *Circ Res* 2006, **98**(7):905-912.
68. Festing MH, Speer MY, Yang HY, Giachelli CM: **Generation of mouse conditional and null alleles of the type III sodium-dependent phosphate cotransporter PIT-1.** *Genesis* 2009, **47**(12):858-863.

doi:10.1186/1471-2091-12-21

**Cite this article as:** Bøttger and Pedersen: Mapping of the minimal inorganic phosphate transporting unit of human Pit2 suggests a structure universal to Pit-related proteins from all kingdoms of life. *BMC Biochemistry* 2011 **12**:21.

**Submit your next manuscript to BioMed Central  
and take full advantage of:**

- Convenient online submission
- Thorough peer review
- No space constraints or color figure charges
- Immediate publication on acceptance
- Inclusion in PubMed, CAS, Scopus and Google Scholar
- Research which is freely available for redistribution

Submit your manuscript at  
www.biomedcentral.com/submit

